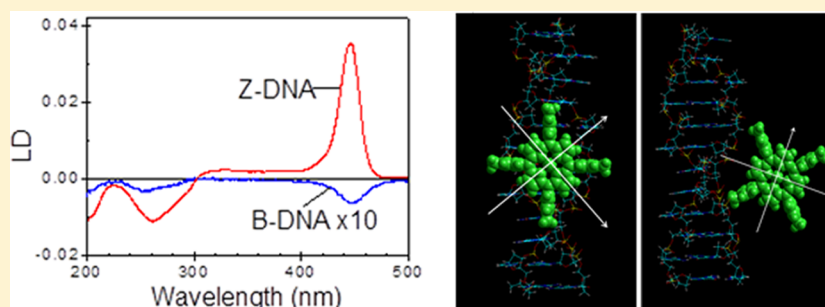


Z-Form DNA Specific Binding Geometry of Zn(II) *meso*-Tetrakis(*N*-methylpyridinium-4-yl)porphyrin Probed by Linear Dichroism SpectroscopyLindan Gong,<sup>†</sup> Yoon Jung Jang,<sup>†</sup> Jinheung Kim,<sup>‡</sup> and Seog K. Kim<sup>\*,†</sup><sup>†</sup>Department of Chemistry, Yeungnam University Dae-dong, Gyeongsan City, Gyeong-buk, 712-749, Republic of Korea<sup>‡</sup>Department of Chemistry and Nano Science, Ewha Womans University, Seoul 120-750, Republic of Korea

**ABSTRACT:** Zn(II) *meso*-tetrakis(*N*-methylpyridinium-4-yl)porphyrin (ZnTMPyP) produced a unique linear dichroism (LD) spectrum when forming a complex with Z-form poly[d(G-C)<sub>2</sub>]. The spectrum was characterized by a large positive wavelength-dependent LD signal in the Soret absorption region. The magnitudes of LD in both the DNA and Soret band increased as the [porphyrin]/[DNA base] ratio increased and were larger by 20–40 times compared to the negative LD of the ZnTMPyP bound to B-form poly[d(G-C)<sub>2</sub>] and poly[d(A-T)<sub>2</sub>]. The angles calculated from LD were respectively 49° and 42° for *B<sub>x</sub>* and *B<sub>y</sub>* transitions of the porphyrin with respect to the local helix axis of Z-form poly[d(G-C)<sub>2</sub>]. The appearance of the unique LD spectrum for the Z-form poly[d(G-C)<sub>2</sub>] complex was accompanied by a bisignate circular dichroism spectrum in the Soret region, whose magnitude was proportional to the square of the porphyrin concentration, suggesting a stacking interaction between Z-form poly[d(G-C)<sub>2</sub>]-bound ZnTMPyP with other bound ZnTMPyP. From these observations, a conceivable binding mode of ZnTMPyP to Z-form poly[d(G-C)<sub>2</sub>] complex was proposed, in which ZnTMPyP binds at the major groove or across the groove. In contrast with Z-form poly[d(G-C)<sub>2</sub>], ZnTMPyP binds to poly[d(A-T)<sub>2</sub>] in a monomeric manner with the angles of 57° and 59° for the two porphyrin's transition moments with respect to the local polynucleotide helix axis. The polarized spectral properties of ZnTMPyP bound to B-form poly[d(G-C)<sub>2</sub>] coincide with the intercalated nonmetallic TMPyP, namely, a negative CD signal in the Soret band and a negative wavelength-dependent reduced LD signal, with a magnitude larger than that in the DNA absorption region in spite of its axial ligands.

## ■ INTRODUCTION

Z-DNA has been the subject of intensive study since its zigzag left-handed helix structure was discovered.<sup>1,2</sup> Although Z-DNA has higher energy compared to B-DNA under physiological conditions,<sup>3–5</sup> its biological importance was highlighted by the discovery of Z-DNA specific proteins,<sup>6–10</sup> implying its significant role in various biological processes such as gene regulations.<sup>11–16</sup> Recognition and stabilization of Z-DNA by small molecules with Z-DNA also has been an interesting subject. Although various small molecules including polyamines,<sup>17,18</sup> [Co(NH<sub>3</sub>)<sub>6</sub>]<sup>3+</sup>,<sup>19</sup> poly(L-lysine)-*graft*-dextran,<sup>19</sup> and polynuclear platinum complexes<sup>20</sup> have been known to induce the B → Z transition of poly[d(G-C)<sub>2</sub>], intercalating drugs such as ethidium generally destabilize Z-DNA.<sup>21</sup> 4',6-Diamidino-2-phenylindole, which preferentially binds at the minor groove of continuous AT base pairs of native DNA, was also reported to induce Z → B transition of poly[d(G-m<sup>5</sup>C)<sub>2</sub>].<sup>22</sup> [Ru(dip)<sub>2</sub>dppz]<sup>2+</sup> is a recent example that induces

the B → Z transition.<sup>23</sup> In contrast to the B → Z transition that occurs preferentially in the GC rich region, this Ru(II) complex was strikingly shown to be able to induce sequence-independent B → Z transition.

Cationic porphyrins have been known to bind DNA. They display a wide variety of binding modes including intercalation,<sup>24,25</sup> monomeric minor groove binding,<sup>26–31</sup> and moderate and extensive stacking to B-DNA.<sup>32–35</sup> The binding modes of porphyrins depend on the nature of porphyrin and its periphery substituents, ionic strength of solution, and base sequence of DNAs. Different binding modes associate with their diagnostic induced circular dichroism (referred to as CD) spectra in the Soret band. For example, *meso*-tetrakis(*N*-methylpyridinium-4-yl)porphyrin (herein denoted as TMPyP), a representative

Received: April 30, 2012

Revised: July 3, 2012

Published: July 17, 2012

member of the porphyrin family, intercalates into the GC-rich synthetic polynucleotides or native DNA at a low [porphyrin]/[DNA] ratio and produces a negative CD band.<sup>36</sup> When associated with AT-rich synthetic polynucleotide, TMPyP binds at the minor groove producing a positive CD band at low [porphyrin]/[DNA] ratios whereas they stack or form an assembly along the major groove of AT-rich polynucleotides or native DNA at high [porphyrin]/[DNA] ratios. The latter binding mode produces a bisignate CD spectrum in the Soret band.<sup>37–39</sup> Recently, these CD properties of porphyrin were used for chiroptical detection of Z-form DNA. Anionic Ni(II) *meso*-tetrakis(4-sulfonatophenyl)porphyrin was able to detect the Z-form DNA in the Z-DNA/B-DNA mixture by inducing a strong bisignate CD in the Soret band.<sup>40,41</sup> Association of anionic porphyrin to negatively charged DNA was an astonishing observation. ZnTMPyP (Figure 1) also bound to Z-DNA and produced a strong bisignate CD spectrum, suggesting electronic coupling between the Z-form DNA-bound ZnTMPyP, differed from the B-form DNA.<sup>42,43</sup>

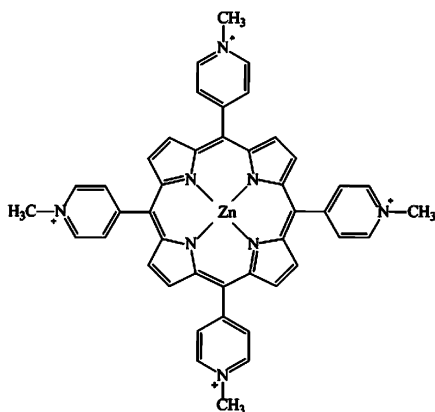


**Figure 1.** Molecular structure of Zn(II) *meso*-tetrakis(*N*-methylpyridinium-4-yl)porphyrin (ZnTMPyP).

In this study, we compared the binding geometry of ZnTMPyP bound to the B- and Z-forms of poly[d(G-C)<sub>2</sub>] by polarized spectroscopic techniques including circular and linear dichroism spectroscopies (CD and LD, respectively). The binding geometry of ZnTMPyP bound to Z-form poly[d(G-C)<sub>2</sub>] was unique and was in sharp contrast with that bound to B-form polynucleotides. Furthermore, the spectral characteristics of the Z-poly[d(G-C)<sub>2</sub>]-ZnTMPyP was also compared with those of the poly[d(A-T)<sub>2</sub>]-ZnTMPyP complex because the former complex has been reported to produce a bisignate CD spectrum in the Soret absorption region,<sup>42,43</sup> similarly to that of the latter complex.

## MATERIALS AND METHODS

**Materials.** Poly[d(G-C)<sub>2</sub>] was purchased from Sigma. It was dissolved in 5 mM cacodylate buffer, pH 7.0 and used without further purification. ZnTMPyP was purchased from Frontier Scientific (Logan, Utah). The concentrations were determined spectrophotometrically using extinction coefficients  $\epsilon_{257\text{nm}} = 8400 \text{ M}^{-1} \text{ cm}^{-1}$  for poly[d(G-C)<sub>2</sub>],  $\epsilon_{262\text{nm}} = 8400 \text{ M}^{-1} \text{ cm}^{-1}$  for poly[d(A-T)<sub>2</sub>], and  $\epsilon_{436\text{nm}} = 204\,000 \text{ M}^{-1} \text{ cm}^{-1}$  for ZnTMPyP. The Z-form of poly[d(G-C)<sub>2</sub>] was stabilized by mixing of spermine and poly[d(G-C)<sub>2</sub>]<sup>17</sup> in 5 mM cacodylate buffer, pH = 7.0. Final concentrations in the mixture were 100 and 18  $\mu\text{M}$  for poly[d(G-C)<sub>2</sub>] and spermine, respectively. This mixture was

incubated at 60 °C for 15 min and cooled to room temperature. Formation of Z-form was ensured by its CD spectrum.

**Measurements.** CD spectra were obtained using either a JASCO J-715 or a J-810 spectropolarimeter (Tokyo, Japan). Absorption spectra were recorded using a Cary 100 spectrophotometer (Palo Alto, CA). Linear dichroism (LD) spectra were measured using a JASCO 715 spectropolarimeter equipped with a flow-orienting Couvette cell device with inner-rotating cylinder as it was described elsewhere.<sup>44–46</sup> The reduced linear dichroism (herein referred to as LD<sup>r</sup>) obtained by division of the measured LD spectrum by isotropic absorption spectrum is related to the orientation factor, *S*, and the angle,  $\alpha$ , through eq 1.

$$\text{LD}^r = 1.5S(3 \cos^2 \alpha - 1) \quad (1)$$

The orientation factor reflects the ability of DNA orientation in the flow, which is affected by the contour length and flexibility of DNA, temperature, and the viscosity of the medium.  $\alpha$  is the angle of the transition moment of the DNA-bound molecule with respect to the local helix axis of the DNA. The orientation factor, *S*, can be calculated by assuming an average angle of 86° between the DNA base plane and the local DNA helix axis, and an LD<sup>r</sup> value of 260 nm.

## RESULTS

**Absorption and CD Spectra.** The binding of ZnTMPyP to poly[d(A-T)<sub>2</sub>] resulted in a 10% increase in absorbance with 1 nm blue shift to 436 nm at its maximum wavelength (Figure 2a). The absorption spectrum was invariant of the mixing ratio, [ZnTMPyP]/[polynucleotide base], which ranged from 0.02 to 0.10, suggesting a homogeneous binding mode of ZnTMPyP to poly[d(A-T)<sub>2</sub>]. In contrast, the binding of ZnTMPyP to poly[d(G-C)<sub>2</sub>] produced a large change: 11 nm red shift from 437 nm in the absence of DNA and 26% hypochromism in the Soret region at the lowest [ZnTMPyP]/[DNA base] ratio (Figure 2b). A small increase in the absorbance and ca. 2 nm blue shift resulted upon increasing the [ZnTMPyP]/[DNA base] ratio. This change was accompanied by an isosbestic point at 449 nm. Thus, in the B-form poly[d(G-C)<sub>2</sub>] case, change in the absorption spectrum suggested that ZnTMPyP intercalates between the DNA base pairs. Two or more ZnTMPyP species in the intercalation site may be involved. Variation of the absorption spectrum of ZnTMPyP that bound to Z-form poly[d(G-C)<sub>2</sub>] was the most drastic (Figure 2c). The absorption maximum was found at 439 nm with 12% hypochromism at the lowest [ZnTMPyP]/[DNA base] ratio compared to that in the absence of DNA. Increasing the ZnTMPyP population produces additional red shift and hyperchromism. An absorption maximum at 442 nm was observed at the highest [ZnTMPyP]/[DNA base] ratio of 0.1. Two isosbestic wavelengths were found for the relative concentration-dependent absorption spectrum of the Z-form poly[d(G-C)<sub>2</sub>]-ZnTMPyP complex, suggesting the presence of at least two or more bound ZnTMPyP species.

CD spectra of ZnTMPyP bound to various polynucleotides are depicted in Figure 3. When associated with poly[d(A-T)<sub>2</sub>], ZnTMPyP produced a complex CD spectrum with two positive maxima at 426 and 448 nm, and a negative minimum at 437 nm (Figure 3a). The shape and intensity were invariant of the [ZnTMPyP]/[DNA base] ratio, suggesting that the binding mode is homogeneous in the concentration range adopted in this study, which is in accordance with the absorption

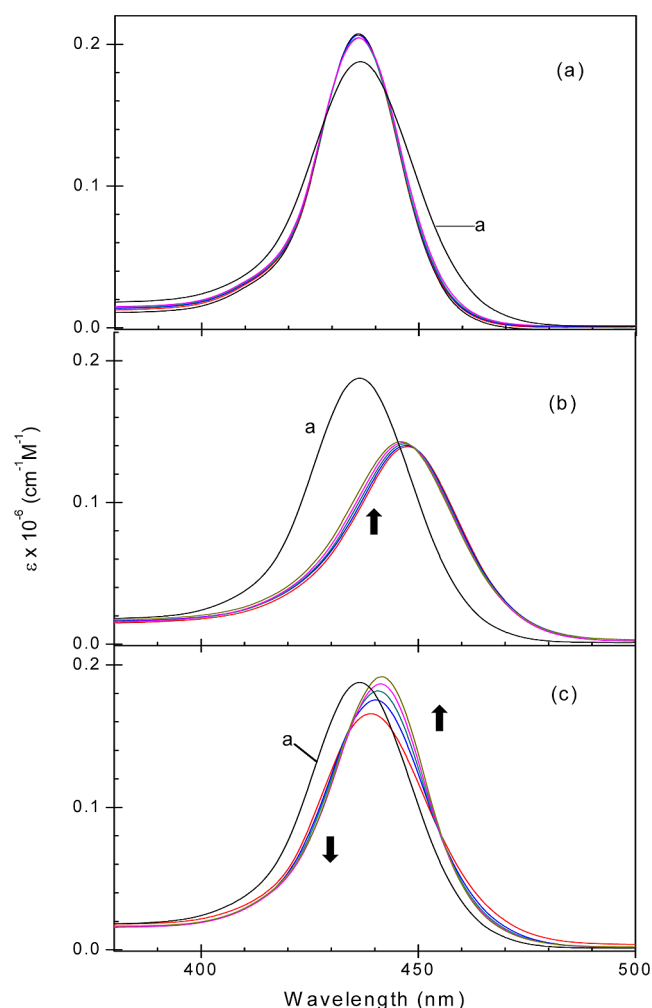


**Figure 2.** Absorption spectrum of Zn(II)TMPyP complexed with B-poly[d(A-T)<sub>2</sub>] (a) and poly[d(G-C)<sub>2</sub>] (b), and Z-form poly[d(G-C)<sub>2</sub>] (c) at various binding ratios in the Soret absorption region. [Polynucleotide] = 100 μM in the base and [porphyrin] = 2, 4, 6, 8, and 10 μM. The [porphyrin]/[polynucleotide] ratio increases along the arrow direction. Polynucleotide-free ZnTMPyP is also shown as a black curve denoted by “a”.

measurement. Appearances of CD spectra of ZnTMPyP complexed with B- and Z-form poly[d(G-C)<sub>2</sub>] shown in Figure 3b,c, respectively, are in agreement with those already reported.<sup>42,43</sup> A negative CD band with its center at 449 nm was observed in the Soret region for ZnTMPyP that was associated with B-form poly[d(G-C)<sub>2</sub>]. The negative CD band in the Soret region has been considered as a diagnostic for intercalated porphyrins.<sup>31,36</sup> As the [ZnTMPyP]/[DNA base] ratio increased, some positive contribution at ca. 429 nm was apparent: the resulting CD spectrum can be considered to be a bisignate, suggesting an interaction or coupling of the electric transition moment between B-form poly[d(G-C)<sub>2</sub>] bound ZnTMPyP. CD spectra of the Z-form poly[d(G-C)<sub>2</sub>]-ZnTMPyP complex are depicted in Figure 3c. The appearance of the CD spectrum of the Z-form poly[d(G-C)<sub>2</sub>]-ZnTMPyP complex was in sharp contrast to the B-form polynucleotides as it was reported.<sup>42</sup> In contrast with the negative weak CD spectrum of the B-form poly[d(G-C)<sub>2</sub>]-ZnTMPyP complex, that of the Z-form poly[d(G-C)<sub>2</sub>]-ZnTMPyP complex was bisignate with its positive maximum at 434 nm and negative minimum at 448 nm even at the lowest [ZnTMPyP]/[DNA

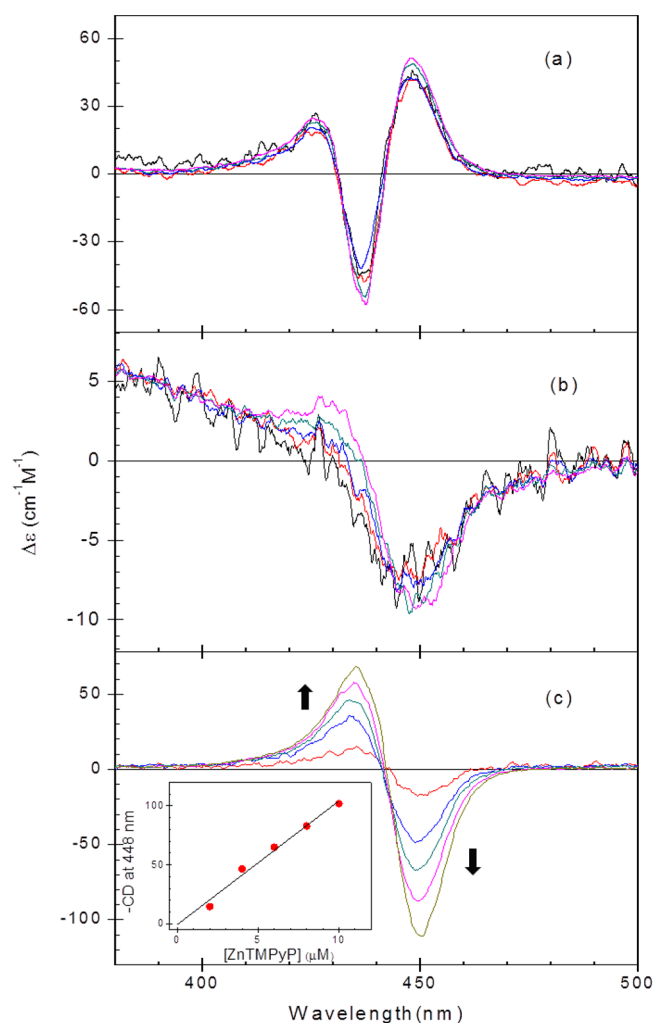


**Figure 3.** CD spectrum of ZnTMPyP complexed with B-form poly[d(A-T)<sub>2</sub>] (a) and poly[d(G-C)<sub>2</sub>] (b), and Z-form poly[d(G-C)<sub>2</sub>] (c) at various binding ratios in the Soret absorption region. The concentrations of ZnTMPyP and polynucleotides are the same as in Figure 2. The inset figure in (c) is the CD intensity ( $\Delta\epsilon$ ,  $\text{cm}^{-1} \text{M}^{-1}$ ) unit at 444 nm of the ZnTMPyP bound to Z-form poly[d(G-C)<sub>2</sub>]. Note that the measured CD intensity was proportional to the square of the porphyrin concentration.

base] ratio of 0.02, or one porphyrin per 50 base pairs. The shape of the CD spectrum of the Z-form poly[d(G-C)<sub>2</sub>]-ZnTMPyP complex was also in contrast with the bisignate CD spectrum observed for the B-form poly[d(A-T)<sub>2</sub>]-ZnTMPyP complex: the negative CD band was observed at long wavelength whereas the positive CD signal was at short wavelength. The most significant difference is the porphyrin concentration dependence. Although the CD spectra for the ZnTMPyP complexed with both the B-form poly[d(G-C)<sub>2</sub>] and poly[d(A-T)<sub>2</sub>] were invariant of the concentration, an increase in the porphyrin population resulted in a drastic increase in the CD intensity for that bound to Z-poly[d(G-C)<sub>2</sub>]. When the CD intensity at 448 nm was plotted with respect to the porphyrin concentration, a straight line was found (Figure 3c, inset). It should be noted that the unit of the CD intensity in the insertion is  $\Delta\epsilon$  ( $\text{cm}^{-1} \text{M}^{-1}$ ). Thus, proportionality in the CD intensity relative to the concentration means that measured CD intensity is proportional to the square of the porphyrin concentration, suggesting that the

formation of excitonic CD was related to the association of two porphyrins.

**LD and LD<sup>r</sup>.** Figure 4 shows the LD spectra of ZnTMPyP complexed with poly[d(A-T)<sub>2</sub>] (panel a), B-form poly[d(G-C)<sub>2</sub>] (panel b), and Z-form poly[d(G-C)<sub>2</sub>] (panel c). The concentrations are the same as in Figure 2.

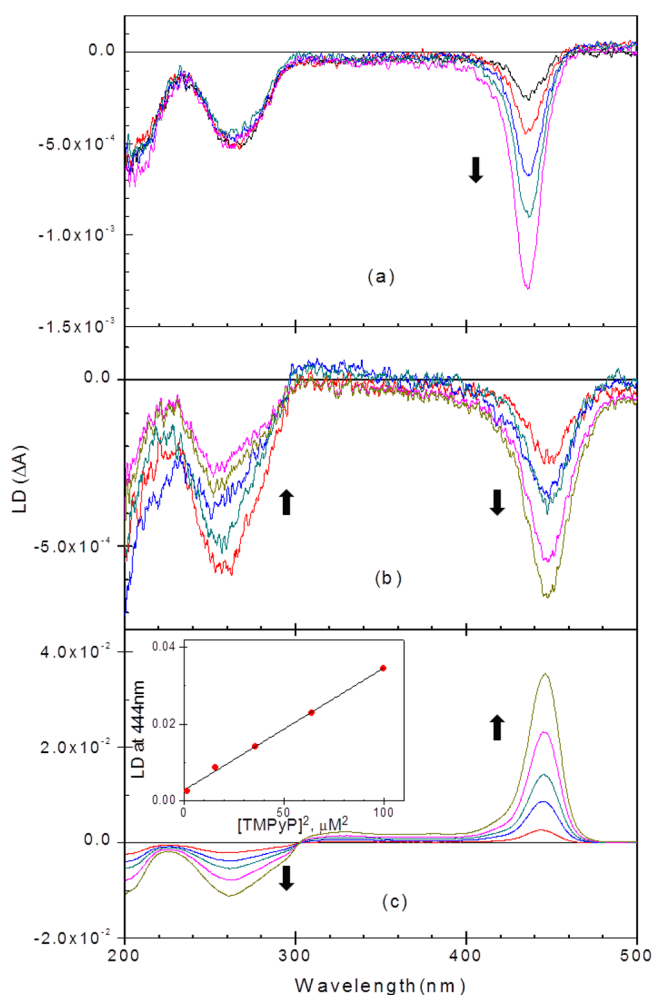


**Figure 4.** LD spectra of ZnTMPyP bound to B-form poly[d(A-T)<sub>2</sub>] (a), poly[d(G-C)<sub>2</sub>] (b), and Z-form poly[d(G-C)<sub>2</sub>] (c). The concentrations are the same as in Figure 2.

C)<sub>2</sub>] (panel b), and Z-form poly[d(G-C)<sub>2</sub>] (panel c), respectively, at various [ZnTMPyP]/[DNA base] ratios. In addition to the CD spectra, the LD spectrum showed striking contrast between Z-form poly[d(G-C)<sub>2</sub>] and B-form poly[d(G-C)<sub>2</sub>], and poly[d(A-T)<sub>2</sub>]. Negative LD bands centered at ca. 260 nm were observed for all three complexes, which were expected from the setup adopted in this study.<sup>44,45</sup> The magnitude of LD in the Soret region centered at 435 nm increased proportionally to the porphyrin concentration whereas it remained in the DNA absorption region in the poly[d(A-T)<sub>2</sub>]-ZnTMPyP complex case. Similarly, negative LD signal in both the DNA and the Soret absorption regions were found for the B-form poly[d(G-C)<sub>2</sub>]-ZnTMPyP complex (Figure 4b). The minimum in LD was at ~447 nm at the lowest [porphyrin]/[DNA base] ratio, which shifted a little to ~445 nm at the highest ratio. Decreases in the LD magnitude in the DNA absorption region and the increases in the Soret region upon increasing ZnTMPyP concentration were observed. However, the Z-form poly[d(G-C)<sub>2</sub>]-ZnTMPyP complex produced a positive LD signal in the Soret region

(Figure 4c). Similarly with CD spectrum, the maximum at ~444 nm was proportional to the square of the porphyrin concentration (Figure 4c, inset). It is noteworthy that the magnitude of the LD spectrum in both the DNA and Soret absorption regions of the Z-form poly[d(G-C)<sub>2</sub>]-ZnTMPyP complex was larger by 20–40 times compared to those of the B-form polynucleotides. Furthermore, the sign of LD in the Soret region was opposite. Hence, LD can be considered as a selective recognizing tool for Z-form poly[d(G-C)<sub>2</sub>] (Figure 5).

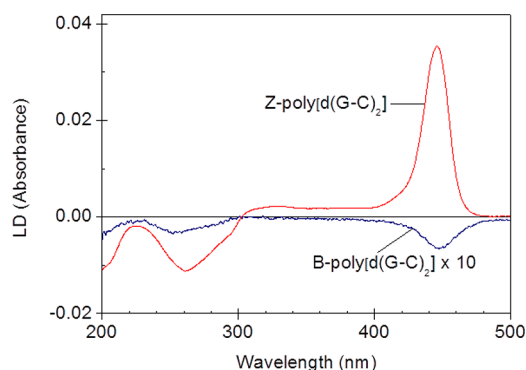


**Figure 5.** Comparison of LD spectrum of the ZnTMPyP complexed with B- and Z-form poly[d(G-C)<sub>2</sub>]. [Polynucleotide] = 100 μM in base and [porphyrin] = 10 μM. The LD signal of the B-form poly[d(G-C)<sub>2</sub>]-ZnTMPyP complex was 10 times enlarged for easy comparison.

Measured LD spectra were divided by absorption spectra to obtain the LD<sup>r</sup> spectrum and the resulting LD<sup>r</sup> spectra are depicted in Figure 6. LD<sup>r</sup> in Figure 6 represent the lowest and highest [porphyrin]/[DNA base] ratios, and corresponding polynucleotides in the absence of ZnTMPyP to avoid complication. Those measured for intermediate [porphyrin]/[DNA base] ratios lie between these two extremes. In both the poly[d(A-T)<sub>2</sub>] and B-form poly[d(G-C)<sub>2</sub>] cases, increasing the porphyrin population caused decreases in the LD<sup>r</sup> magnitude of DNA, as shown in panels a and b, respectively, suggesting that binding of porphyrin induced either increased flexibility or bend of the DNA stem, or both. In the Soret region, the poly[d(A-T)<sub>2</sub>]-ZnTMPyP complex exhibited some wavelength-dependent shape. The magnitude is invariant of the [porphyrin]/[DNA base] ratio and is smaller than that in the DNA absorption region, suggesting that porphyrin's molecular plane tilts to a large extent with respect to the DNA helix axis. On the other hand, a tilted LD<sup>r</sup> with its magnitude larger than that in the DNA absorption region was observed for the poly[d(G-C)<sub>2</sub>]-ZnTMPyP complex. Larger or comparable LD<sup>r</sup> magnitude in the drug's absorption region compared to in the DNA absorption region is typical for intercalated drugs.<sup>47</sup> The appearance of LD<sup>r</sup> spectrum of the Z-form poly[d(G-C)<sub>2</sub>]-ZnTMPyP complex was in sharp contrast with those of the B-form polynucleotides. Upon increasing the [porphyrin]/[DNA] ratio, the LD<sup>r</sup> magnitude in the DNA absorption region increased, suggesting that the binding of ZnTMPyP to Z-form poly[d(G-C)<sub>2</sub>] resulted in either the stiffening or lengthening of the DNA stem, or both. The shape of the LD<sup>r</sup> spectrum in the Soret band is even more spectacular: The LD<sup>r</sup> spectrum appeared to be positive in the entire Soret region and was strongly wavelength-dependent. The positive LD<sup>r</sup> magnitude in the Soret absorption region implies that the



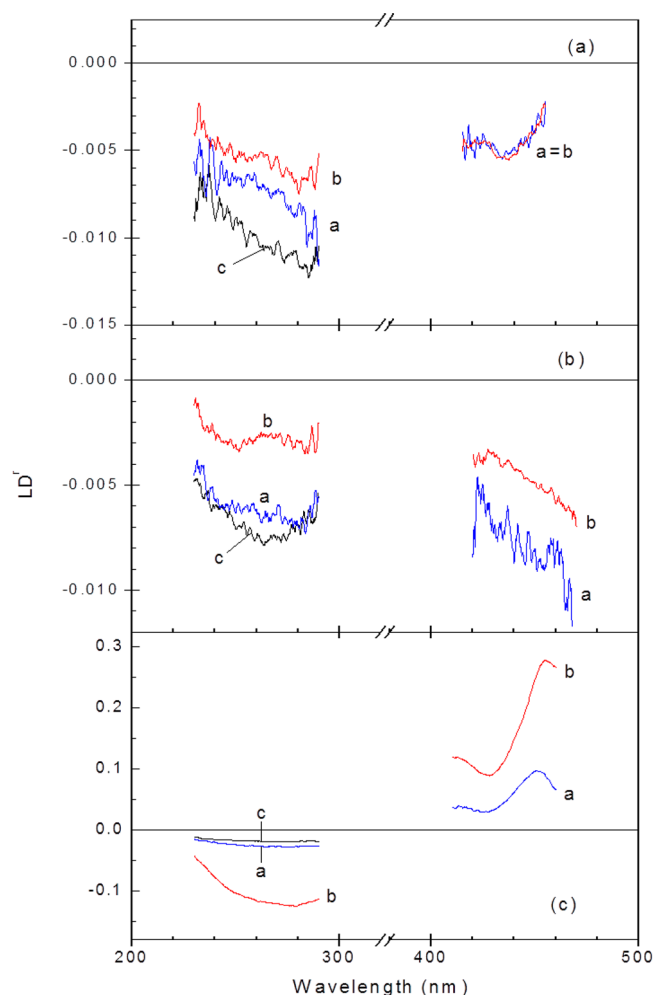


**Figure 6.** Representative LD<sup>r</sup> spectra of the ZnTMPyP complexed with B-form poly[d(A-T)<sub>2</sub>] (a) and poly[d(G-C)<sub>2</sub>] (b), and Z-form poly[d(G-C)<sub>2</sub>] (c). Curves a and b denote the LD<sup>r</sup> spectrum for the [ZnTMPyP]/[DNA base] ratios 0.02 and 0.10, respectively. Curve c represents the corresponding polynucleotide in the absence of porphyrin. [Polynucleotide] = 100 μM.

molecular plane of porphyrin is close to perpendicular with respect to the local DNA helix axis.

**Analysis of LD<sup>r</sup>.** The absorption and LD spectrum in the Soret absorption band consisted of two originally degenerated electric transition moments, namely B<sub>x</sub> and B<sub>y</sub> transitions. The degeneracy of these two transitions can be, at least partially, removed due to different interaction and binding angles relative to the DNA local helix axis. Thus, pure contribution of one of the transitions, e.g., the B<sub>x</sub> transition, in the LD spectrum can be obtained by stepwise reduction of the absorption spectrum multiplied by the properly tuned absorption spectrum.<sup>36,39,48</sup>

$$LD_{B_x}(\lambda) = LD(\lambda) - \kappa A(\lambda) \quad (2)$$

One of the examples for such reduction is presented in Figure 7a for the Z-form poly[d(G-C)<sub>2</sub>]-ZnTMPyP complex at the [porphyrin]/[DNA base] ratio of 0.1. In this particular case, the factor,  $\kappa$ , varies from 0.05 to 0.12 with an increment of 0.01.

The LD spectrum obtained from  $\kappa = 0.08$  was considered as the representative of LD<sub>B<sub>x</sub></sub>(λ). The LD corresponding to the B<sub>y</sub> transition can be obtained from the reduction of LD<sub>B<sub>x</sub></sub>(λ) from the measured LD spectrum. The measured LD spectrum and

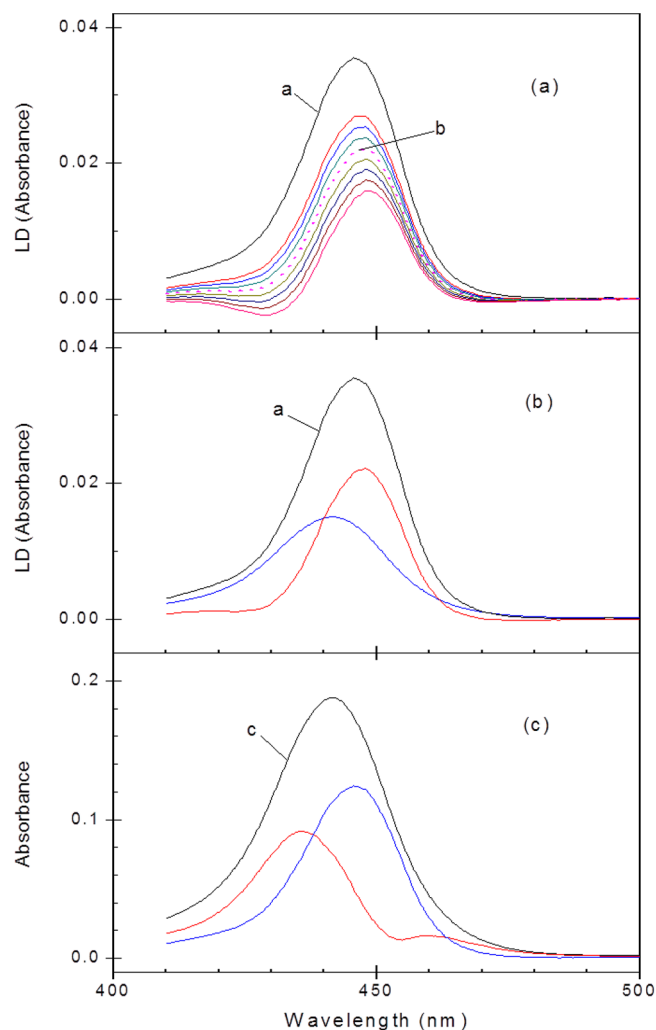


**Figure 7.** (a) Different spectra LD(λ) − κA(λ) of ZnTMPyP bound to Z-form poly[d(G-C)<sub>2</sub>]. [Porphyrin] = 10 μM and [polynucleotide] = 100 μM. The κ values varied between 0.05 and 0.12 with an increment of 0.01. The measured LD spectrum is denoted by “a”. The LD spectrum denoted by “b” (red, dotted curve) was chosen to be the best LD spectrum representing the transition moment B<sub>y</sub> in this particular case (κ = 0.08). (b) and (c) show LD and absorption spectrum resolved into two electric transition moments, namely B<sub>x</sub> (short wavelength) and B<sub>y</sub> (long wavelength) transitions, of ZnTMPyP. See text for explanation.

those that represent B<sub>x</sub> and B<sub>y</sub> transitions are depicted in Figure 7b. In a similar method, the measured absorption spectrum can be resolved through the sum of two absorption spectra, representing B<sub>x</sub> and B<sub>y</sub> transitions (Figure 7c). From these results, LD<sup>r</sup> values representing the B<sub>x</sub> and B<sub>y</sub> transition can be calculated and consequently the angle of each electric transition with respect to the local DNA helix axis was calculated according to eq 1. The angles of B<sub>x</sub> and B<sub>y</sub> transitions of the poly[d(A-T)<sub>2</sub>]-ZnTMPyP complex were 56° and 57°, respectively, relative to the DNA helix axis at the [porphyrin]/[DNA base] ratio of 0.02. Angles obtained from higher mixing ratio were almost identical. Even at the highest mixing ratios ([porphyrin]/[DNA base] = 0.1), the angles were 57° and 59°, suggesting that the binding geometry of ZnTMPyP to poly[d(A-T)<sub>2</sub>] is invariant with respect to the [porphyrin]/[DNA base] ratio adopted in this study (<0.1). In the B-form poly[d(G-C)<sub>2</sub>]-ZnTMPyP complex case, in which the LD<sup>r</sup>

magnitude in the Soret band was larger than in the DNA absorption region, this type of calculation was impossible, because imaginary numbers were involved in the calculation. On the other hand, the angle of the  $B_x$  and  $B_y$  transitions of ZnTMPyP bound to Z-form poly[d(G-C)<sub>2</sub>] were 49° and 42° with respect to the local DNA helix axis, respectively. This observation suggested that the molecular plane of ZnTMPyP tilted toward the DNA helix axis in large extent. As the [porphyrin]/[DNA base] ratio increased, the angle became smaller, 27° and 24° at the highest ratio, suggesting that the molecular plane of ZnTMPyP was close to the DNA helix axis. The angles calculated for intermediate ratios lie between these two extremes.

## DISCUSSION

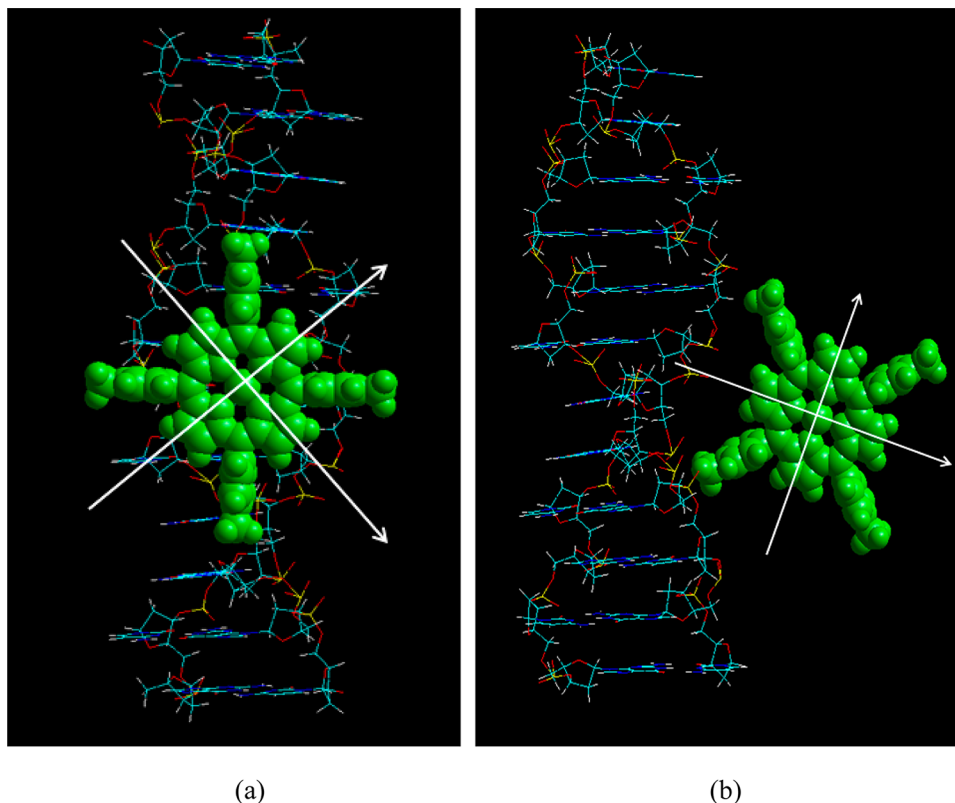
**ZnTMPyP Bound to B-Form Poly[d(G-C)<sub>2</sub>] and Poly[d(A-T)<sub>2</sub>].** Spectral properties of ZnTMPyP bound to poly[d(A-T)<sub>2</sub>] can be summarized as hyperchromism in the absorption spectrum, and a complex CD spectrum in the Soret region and the negative LD<sup>r</sup> spectrum. All these spectral properties were invariant of the [porphyrin]/[DNA base] ratio, indicating that the binding mode of ZnTMPyP was not affected by the relative population of porphyrin adopted in this study, which was below one ZnTMPyP molecule per 10 DNA bases. In other words, any interaction including  $\pi$ - $\pi$  stacking between poly[d(A-T)<sub>2</sub>]-bound ZnTMPyP, including moderate and extensive stacking, was negligible in spite of its bisignate CD spectrum, which has been usually accounted for by the stacking interaction.<sup>36–38</sup> Therefore, the observed bisignate CD spectrum is conceivably the result of different interactions of ZnTMPyP's  $B_x$  and  $B_y$  transitions with chirally arranged DNA bases. The angles in a range of 56–59° for the  $B_x$  and  $B_y$  transitions of ZnTMPyP with respect to the local DNA helix were also invariant of the mixing ratio. The possibility of an intercalative binding mode for ZnTMPyP to poly[d(A-T)<sub>2</sub>] can be definitively ruled out from the calculated binding geometry, leaving the DNA grooves as possible binding sites. Whether the binding site is the major groove or minor groove is unclear from the present spectral results. However, when TMPyP, the same cationic porphyrin without a central Zn ion, binds to DNA or poly[d(A-T)<sub>2</sub>], angles of 74° and 55° for  $B_x$  and  $B_y$  transitions relative to the local DNA helix axis were reported. By combination of these binding angles with other evidence, TMPyP was concluded to bind across the minor groove of DNA.<sup>39</sup>

Intercalative binding of cationic porphyrin has also been reported. Cationic porphyrins, especially TMPyP, has been well-known to intercalate between poly[d(G-C)<sub>2</sub>] or DNA base pairs at low [porphyrin]/[DNA base] ratios.<sup>24,25</sup> Intercalation of TMPyP favors 5'CG3' sites. Intercalated TMPyP is characterized by a large red shift and hypochromism in the absorption spectrum, a negative CD band, and negative LD spectrum in the Soret region. The magnitude of the LD<sup>r</sup> spectrum in the Soret region is larger than that in the DNA absorption region and is strongly wavelength-dependent. Upon increasing the amount of intercalated porphyrins, the magnitude of LD<sup>r</sup> in the DNA absorption region shows a tendency to decrease, indicating that the DNA base plane tilts considerably toward the DNA helix axis. The wavelength-dependent LD<sup>r</sup> in Soret region suggests that the tilt angles of the  $B_x$  and  $B_y$  transitions of TMPyP relative to the DNA helix axis are different, implying that the molecular plane of porphyrin is skewed in the intercalation pocket. All these spectral properties coincide with those observed for the B-form

poly[d(G-C)<sub>2</sub>]-ZnTMPyP complex investigated in this study, indicating strongly that ZnTMPyP is intercalated. In the intercalation pocket, the axial water ligand of the central Zn ion was shown to be removed prior to intercalation.<sup>49,50</sup>

**Z-Form Poly[d(G-C)<sub>2</sub>] Specific Binding Properties of ZnTMPyP.** The spectral properties of ZnTMPyP bound to Z-form poly[d(G-C)<sub>2</sub>] were in contrast with those of ZnTMPyP bound to B-form poly[d(G-C)<sub>2</sub>] and poly[d(A-T)<sub>2</sub>] in various aspects. The pattern of changes in the absorption spectrum of ZnTMPyP upon binding to Z-form poly[d(G-C)<sub>2</sub>] was in contrast with that intercalated to poly[d(G-C)<sub>2</sub>] and that bound outside of poly[d(A-T)<sub>2</sub>]. A bisignate CD spectrum in the Soret band was apparent for the Z-form poly[d(G-C)<sub>2</sub>]-ZnTMPyP complex which is in agreement with a previous report.<sup>42</sup> Although the appearance of a CD spectrum of the Z-form poly[d(G-C)<sub>2</sub>]-ZnTMPyP complex was comparable with that bound to poly[d(A-T)<sub>2</sub>] in a sense that both are bisignate, the intensity of the CD spectrum of the former appeared dependent on the square of the porphyrin concentration whereas the latter was linearly proportional. Thus, in the poly[d(A-T)<sub>2</sub>]-bound ZnTMPyP case, the bisignate CD spectrum was conceivably due to the different interaction of the two transitions in the Soret band with chirally arranged AT bases. On the other hand, ZnTMPyP bound to Z-form poly[d(G-C)<sub>2</sub>] interacted with other bound ZnTMPyP, and that interaction involved two ZnTMPyPs. The stacking interaction of porphyrin bound to DNA or polynucleotide producing a bisignate CD is well-known.<sup>37–39</sup> A through space exciton coupling for originally observed bisignate CD spectrum was proposed by Balaz and his co-workers.<sup>42</sup> Although the electric coupling occurs between the porphyrins that are either stacked or apart is not clear at this stage, the fact that an increase in the magnitude of bisignate CD is proportional to the square of the porphyrin concentration may be considered as an conceivable evidence for the dimeric interaction.

The magnitudes of negative LD and LD<sup>r</sup> of B-form polynucleotides in the DNA absorption region decreased upon increasing the ZnTMPyP population. The decrease in the LD intensity in this wavelength region (~260 nm) may be due to either bending of the DNA stem or the positive contribution from DNA-bound ZnTMPyP. Considering that the absorbance of porphyrins in the DNA absorption region is small, the decrease in the LD magnitude for both B-forms of poly[d(A-T)<sub>2</sub>] and poly[d(G-C)<sub>2</sub>] reflects, at least in part, the bending of DNA upon ZnTMPyP binding. In contrast, the LD magnitude of Z-form poly[d(G-C)<sub>2</sub>] was greater compared to the B-form, reflecting the decreased flexibility of the Z-form poly[d(G-C)<sub>2</sub>] stem.<sup>22</sup> Addition of ZnTMPyP resulted in a further increase (Figures 4), indicating that the Z-form poly[d(G-C)<sub>2</sub>] became stiffer as a result of ZnTMPyP binding. The possibility of intercalative binding mode for ZnTMPyP to Z-form poly[d(G-C)<sub>2</sub>] can be rejected from the angles of 49° and 42° for  $B_x$  and  $B_y$  transitions with respect to the local DNA helix axis at the lowest [ZnTMPyP]/[DNA base] ratio. The minor groove of Z-form poly[d(G-C)<sub>2</sub>] is narrow and deep. If the side of the ZnTMPyP molecule inserts into the narrow groove, the observed angle may be possible. However, if the porphyrin molecule is inserted into the groove, the stacking interaction that was evident by CD measurement cannot be explained, because the porphyrin molecule must situate in a head-to-tail arrangement in the groove. Furthermore, spermine has been reported to situate in the minor groove of Z-form DNA,<sup>51,52</sup> mediating contacts between neighboring duplex. The occupa-

Scheme 1. Possible Binding Geometry for ZnTMPyP Bound to Z-Form Poly[d(G-C)<sub>2</sub>]<sup>a</sup>

<sup>a</sup>In (a), the molecular plane of porphyrin faces the center of polynucleotide, whereas the porphyrin molecule binds across the groove in (b).

tion of the minor groove by spermine prevents the incoming of the side of the ZnTMPyP, ruling out the possibility of the minor groove binding mode. Another conceivable possibility is that ZnTMPyP binds to the major groove of Z-form poly[d(G-C)<sub>2</sub>], which is wide and shallow. In this groove, there are two ways for ZnTMPyP to bind to Z-form poly[d(G-C)<sub>2</sub>]: the molecular plane of porphyrin either parallel or perpendicular to the DNA helix axis (Scheme 1). In both binding modes, the angle of the two transitions relative to the polynucleotide helix axis can be close to the measured values of 49° and 42°. In the former case, the molecular plane of porphyrin faces to the center of polynucleotide, whereas the porphyrin molecule sits across the groove in the latter case. Electrostatic interaction between the positive charges of ZnTMPyP and the negative charges of polynucleotide's phosphate group may be the major interaction in both binding modes. This binding geometry can also provide room for the second ZnTMPyP to stack.

## CONCLUSION

ZnTMPyP forms a complex with Z-form poly[d(G-C)<sub>2</sub>]. In the complex, it conceivably binds at the major groove and is stabilized mainly by the electrostatic interaction between the phosphate groups of polynucleotide and the positive charges of the porphyrins. Z-form poly[d(G-C)<sub>2</sub>]-bound ZnTMPyP produced a unique large positive LD signal in the Soret region with its magnitude larger by 20–40 times compared to that of negative LD for the complex formed with B-form polynucleotide.

## AUTHOR INFORMATION

### Corresponding Author

\*E mail: seogkim@yu.ac.kr. Tel: +82 53 810 2362. Fax: +82 53 815 5412.

### Notes

The authors declare no competing financial interest.

## ACKNOWLEDGMENTS

This study was supported by the Korea Research Foundation (Grant nos. 2009-0087304 and 2011-0014336).

## REFERENCES

- (1) Pohl, F. M.; Jovin, T. M. *J. Mol. Biol.* **1972**, *7*, 375–396.
- (2) Wang, A. H.-J.; Quigley, G. J.; Kolpak, F. J.; Crawford, J. L.; Van Boom, J. H.; Van der Marel, G.; Rich, A. *Nature* **1979**, *282*, 680–686.
- (3) Jovin, T. M.; Soumpasis, D. M.; McIntoch, L. P. *Annu. Rev. Phys. Chem.* **1987**, *38*, 521–560.
- (4) Rich, A.; Nordheim, A.; Wang, A. H.-J. *Annu. Rev. Biochem.* **1984**, *53*, 791–846.
- (5) Rich, A.; Zhang, S. *Nat. Rev. Genet.* **2003**, *4*, 566–573.
- (6) Herbert, A.; Alfken, J.; Kim, Y.-G.; Mian, I. S.; Nishimoto, K.; Rich, A. *Proc. Natl. Acad. Sci. U. S. A.* **1997**, *94*, 8421–8426.
- (7) Schwartz, T.; Rould, M. A.; Lowenhaupt, K.; Herbert, A.; Rich, A. *Science* **1999**, *284*, 1841–1845.
- (8) Schwartz, T.; Behlke, J.; Lowenhaupt, K.; Heinemann, U.; Rich, A. *Nat. Struct. Biol.* **2001**, *8*, 761–765.
- (9) Kim, Y.-G.; Muralinath, M.; Brandt, T.; Percy, M.; Hauns, K.; Lowenhaupt, K.; Jacobs, B. L.; Rich, A. *Proc. Natl. Acad. Sci. U. S. A.* **2003**, *100*, 6974–6979.
- (10) Lowenhaupt, K.; Oh, B.-K.; Kim, K. K.; Rich, A. *Proc. Natl. Acad. Sci. U. S. A.* **2004**, *101*, 1514–1518.
- (11) Wittig, B.; Wolff, S.; Dorbic, T.; Vahrson, W.; Rich, A. *EMBO J.* **1992**, *11*, 4653–4663.

- (12) Brandt, T. A.; Jacobs, B. L. *J. Virol.* **2001**, *75*, 850–856.
- (13) Oh, D. B.; Kim, Y. G.; Rich, A. *Proc. Natl. Acad. Sci. U. S. A.* **2002**, *101*, 16666–16671.
- (14) Kwon, J. A.; Rich, A. *Proc. Natl. Acad. Sci. U. S. A.* **2005**, *102*, 12759–12764.
- (15) Takaoka, A.; Wang, Z.; Choi, M. K.; Yanai, H.; Negishi, H.; Ban, T.; Lu, Y.; Miyagishi, M.; Kodama, T.; Honda, K.; et al. *Nature* **2007**, *448*, 501–505.
- (16) Ray, B. K.; Dhar, S.; Shaky, A.; Ray, A. *Proc. Natl. Acad. Sci. U. S. A.* **2011**, *108*, 103–108.
- (17) Parkinson, A.; Hawken, M.; Hall, M.; Sanders, K. J.; Rodger, A. *Phys. Chem. Chem. Phys.* **2000**, *2*, 5469–5478.
- (18) Thomas, T. J.; Gunna, U. B.; Thomas, T. *J. Biol. Chem.* **1991**, *266*, 6137–6141.
- (19) Shimada, N.; Kano, A.; Maruyama, A. *Adv. Funct. Mater.* **2009**, *19*, 3590–3595.
- (20) McGregor, T. D.; Balcarová, Z.; Qu, Y.; Tran, M.-C.; Zaludová, R.; Brabec, V.; Farrell, N. *J. Inorg. Biochem.* **1999**, *77*, 43–46.
- (21) Möller, A.; Nordheim, A.; Kozłowski, S. A.; Patel, D. J.; Rich, A. *Biochemistry* **1984**, *23*, 54–62.
- (22) Kim, S. K.; Eriksson, S.; Nordén, B. *Biopolymers* **1993**, *33*, 1677–1686.
- (23) Wu, Z.; Tian, T.; Yu, J.; Weng, X.; Liu, Y.; Zhou, X. *Angew. Chem., Int. Ed.* **2011**, *50*, 11962–11967.
- (24) Marzilli, L. G.; Banville, L. D.; Wilson, W. D. *J. Am. Chem. Soc.* **1986**, *108*, 4188–4192.
- (25) Guliaev, A. B.; Leontis, N. B. *Biochemistry* **1999**, *38*, 15425–15437.
- (26) Kuroda, R.; Tanaka, H. *J. Chem. Soc., Chem. Commun.* **1994**, 1575–1576.
- (27) Sehlstedt, U.; Kim, S. K.; Carter, P.; Goodisman, J.; Vollano, J. K.; Nordén, B.; Dabrowiak, J. C. *Biochemistry* **1994**, *33*, 417–426.
- (28) Schneider, H. J.; Wang, M. *J. Org. Chem.* **1994**, *59*, 7473–7478.
- (29) Yun, B. H.; Jeon, S. H.; Cho, T.-S.; Yi, Y.; Sehlstedt, U.; Kim, S. K. *Biophys. Chem.* **1998**, *70*, 1–10.
- (30) Lee, S.; Jeon, S. H.; Kim, B. J.; Han, S. W.; Jang, H. G.; Kim, S. K. *Biophys. Chem.* **2001**, *92*, 35–45.
- (31) Lee, S.; Lee, Y. A.; Lee, H. M.; Lee, J. Y.; Kim, D. H.; Kim, S. K. *Biophys. J.* **2002**, *83*, 371–381.
- (32) Marzilli, L. G. *New J. Chem.* **1990**, *14*, 409–420.
- (33) Lipscomb, L. A.; Zhou, F. X.; Presnell, S. R.; Woo, R. J.; Peek, M. E.; Plaskon, R. R.; Williams, L. D. *Biochemistry* **1996**, *35*, 2818–2823.
- (34) Ismail, M. A.; Rodger, P. M.; Rodger, A. J. *Biomol. Struct. Dynam.* **2000**, *Conversation 11*, 335–348.
- (35) Pasternack, R. F. *Chirality* **2003**, *15*, 329–332.
- (36) Lee, Y.-A.; Lee, S.; Cho, T.-S.; Kim, C.; Han, S. W.; Kim, S. K. *J. Phys. Chem. B* **2002**, *106*, 11351–11355.
- (37) Lee, Y.-A.; Kim, J.-O.; Cho, T.-S.; Song, R.; Kim, S. K. *J. Am. Chem. Soc.* **2003**, *125*, 8106–8107.
- (38) Kim, J.-O.; Lee, Y.-A.; Yun, B. H.; Han, S. W.; Kwag, S. T.; Kim, S. K. *Biophys. J.* **2004**, *86*, 1012–1017.
- (39) Jin, B.; Lee, H. M.; Lee, Y.-A.; Ko, J. H.; Kim, C.; Kim, S. K. *J. Am. Chem. Soc.* **2005**, *127*, 2417–2424.
- (40) Choi, J. K.; Sargsyan, G.; Shabbir-Hussain, M.; Holmes, A. E.; Balaz, M. *J. Phys. Chem. B* **2011**, *115*, 10182–10188.
- (41) D'Urso, A.; Mammana, A.; Balaz, M.; Holmes, A. E.; Berova, N.; Lauceri, R.; Purrello, R. *J. Am. Chem. Soc.* **2009**, *131*, 2046–2047.
- (42) Balaz, M.; De Napoli, M.; Holmes, A. E.; Mammana, A.; Nakanishi, K.; Berova, N.; Purrello, R. *Angew. Chem., Int. Ed.* **2005**, *44*, 4006–4009.
- (43) D'Urso, A.; Holmes, A. E.; Berova, N.; Balaz, M.; Purrello, R. *Chem. Asian. J.* **2011**, *6*, 3104–3109.
- (44) Nordén, B.; Kubista, M.; Kurucsev, T. *Q. Rev. Biophys.* **1992**, *25*, 51–170.
- (45) Rodger, A.; Nordén, B. *Circular Dichroism and Linear Dichroism*; Oxford Press: New York, 1997.
- (46) Nordén, B.; Seth, S. *Appl. Spectrosc.* **1985**, *39*, 647–655.
- (47) Tuite, E.; Nordén, B. *Bioorg. Med. Chem.* **1995**, *3*, 701–711.
- (48) Jin, B.; Min, K. S.; Han, S. W.; Kim, S. K. *Biophys. Chem.* **2009**, *144*, 38–45.
- (49) Chirvony, V. S.; Galievsky, V. A.; Terekhov, S. N.; Dzhagarov, B. M.; Ermolenkov, V. V.; Turpin, P. *Biospectroscopy* **1999**, *5*, 302–312.
- (50) Bejune, S. A.; Shelton, A. H.; McMillin, D. R. *Inorg. Chem.* **2003**, *42*, 8465–8475.
- (51) Egli, M.; Williams, L. D.; Gao, Q.; Rich, A. *Biochemistry* **1991**, *30*, 11388–11402.
- (52) Bancroft, B.; Williams, L. D.; Rich, A.; Egli, M. *Biochemistry* **1994**, *33*, 1073–1086.